

AdaFV: Accelerating VLMs with Self-Adaptive Cross-Modality Attention Mixture

Jiayi Han^{1,2}, Liang Du³, Yiwen Wu^{1,2}, Xiangguo Zhou^{1,2},
Hongwei Du^{1,2}, Weibo Zheng^{1,2}

¹Inspur Genersoft Co. Ltd., Inspur Group Co. Ltd.

²Shandong Key Laboratory of Automated Complex Network Software Construction

³Interactive Entertainment Group, Tencent Inc.

Correspondence: hanjiayi@inspur.com

Abstract

The success of VLMs often relies on the dynamic high-resolution schema that adaptively augments the input images to multiple crops, so that the details of the images can be retained. However, such approaches result in a large number of redundant visual tokens, thus significantly reducing the efficiency of the VLMs. To improve the VLMs' efficiency without introducing extra training costs, many research works are proposed to reduce the visual tokens by filtering the uninformative visual tokens or aggregating their information. Some approaches propose to reduce the visual tokens according to the self-attention of VLMs, which are biased, to result in inaccurate responses. The token reduction approaches solely rely on visual cues are text-agnostic, and fail to focus on the areas that are most relevant to the question, especially when the queried objects are non-salient to the image. In this work, we first conduct experiments to show that the original text embeddings are aligned with the visual tokens, without bias on the tailed visual tokens. We then propose a self-adaptive cross-modality attention mixture mechanism that dynamically leverages the effectiveness of visual saliency and text-to-image similarity in the pre-LLM layers to select the visual tokens that are informative. Extensive experiments demonstrate that the proposed approach achieves state-of-the-art training-free VLM acceleration performance, especially when the reduction rate is sufficiently large.

1 Introduction

In recent years, vision-language models (VLMs) have shown extraordinary strength in general visual-grounded tasks, and are widely utilized in image captioning, vision question answering, layout understanding, and other scenarios. Although

the VLMs have achieved great success, the computational cost is a large burden for real utilization. For example, LLaVA-NEXT models (Liu et al., 2024) include 2880 visual tokens for the single image tasks, and modern VLMs like InternVL-2.5 (Chen et al., 2024b) include 8K+ visual tokens for each task, which could be much longer than the text prompts. To deal with this issue, many research works propose to prune the redundant visual tokens for training-free VLM acceleration. For example, FastV (Chen et al., 2024a) analyzes the attention weights within the VLM layers and finds that the distribution of attention weights of the visual tokens significantly drops during feed-forward. The visual tokens are ranked according to the attention weights, and only the top-ranked tokens are reserved. Similarly, SparseVLM (Zhang et al., 2024b) first selects the text tokens that are highly relevant to the visual tokens, then rates the significance of vision tokens within the self-attention matrix corresponding to the selected text tokens, and the irrelevant visual tokens are gradually pruned from the hidden states. FasterVLM (Zhang et al., 2024a) finds that the text-to-image attention weights are biased, and cannot fully reveal the significance of the visual tokens. On the contrary, the visual saliency extracted from the visual encoder could avoid such bias and could be an effective metric for visual token pruning.

In this work, we propose leveraging the effectiveness of text-to-image (T2I) similarity and visual saliency for visual token pruning. First, we analyze the alignment of the visual tokens to the text embeddings in the VLMs. Although FasterVLM (Zhang et al., 2024a) reveals that the self-attention is shifted to the tailed visual tokens thus resulting in the unreliable token selection, we find that the similarity between text embeddings and the visual tokens do not suffer from such misalignment, and capable of locate the prompt-related visual tokens with a smaller token budget. However,

Work on progress

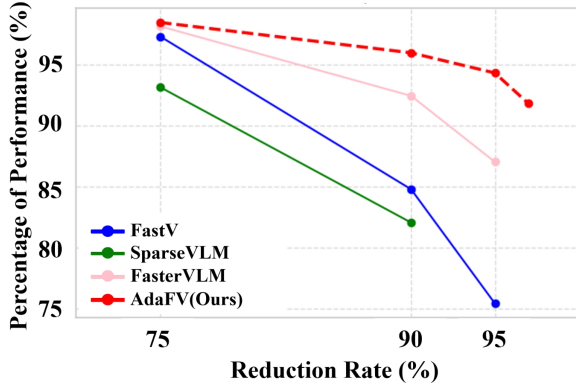


Figure 1: The performance of different training-free VLM acceleration methods on LLaVA-NEXT-7B. Compared with the other state-of-the-art methods, the proposed approach significantly increased the robustness of the model. The proposed approach achieves an above 90% average score across 7 benchmark datasets when the visual token reduction rate is above 95%, which demonstrates the effectiveness of the proposed approach.

there are visual clues that are not suitable for such cross-modality alignment, such as document images. To address such scenarios, we propose a novel self-adaptive cross-modality attention mixture (SACMAM) approach that effectively balances the weight of text-to-image similarity and visual saliency. To ensure the co-dependence on T2I similarity and visual saliency, we measure the overall significance of the selected subset of visual tokens by independent geometric average and utilize a one-step optimization to find the suitable collection.

Extensive experiments demonstrate that the proposed method achieves state-of-the-art performance on multiple benchmark datasets, and could even be comparable to fine-tuning methods such as VisionZip (Yang et al., 2024). Our main contributions are listed as follows:

1. We comprehensively analyze the distribution of text-to-image attention, partially revealing the reason for the inaccuracy of text-to-image attention, and solve by simply introducing cosine similarity.
2. We propose a novel self-adaptive cross-modality attention mixture mechanism (SACMM) that adaptively determines the number of the weight of T2I attention and visual saliency, effectively balancing the strength of text-to-image attention and visual saliency for visual token pruning.

3. Extensive experiments demonstrate that the proposed approach achieves state-of-the-art performance, and is comparable to the fine-tuned methods.

2 Related work

2.1 Vision language models (VLMs)

Notable progress has been for vision language models. LLaVA(Yifan et al., 2023) is the first approach that leverages the effectiveness of LLMs and foundation vision models. Following LLaVA, a series of VLMs are proposed, which brings strong multi-model capacity (Lin et al., 2023; Bai et al., 2023; Chen et al., 2024c). The original LLaVA family models only utilize one image as input, resulting in 576 visual tokens for a 336×336 image. However, this strategy may resulting significant information loss, which degrades the model capacity. To deal with this issue, many VLMs introduce dynamic high-resolution strategies. Despite their success, the high-resolution strategies significantly scaled up the visual tokens. For example, LLaVA-NEXT models (Liu et al., 2024) involve up to 2880 visual tokens for the same task.

2.2 VLM acceleration with token pruning

Token pruning is the most intuitive solution for the acceleration of transformer models. Since the information could be merged to a fewer number of tokens, pruning the redundant tokens could safely accelerate the transformer models, with a slight influence on the model performance, while significantly reducing the computational cost (Kim et al., 2022; Fu et al., 2024b; Wang et al., 2024). Some approaches borrow this finding to accelerate the VLMs. Chen et al. (2024a); Ye et al. (2024) propose to measure the significance of the visual tokens according to the self-attention extracted from within the LLMs. To further accelerate the models, some approaches place this token pruning procedure before the encoder layers of the LLMs. For example, FasterVLM suggests that the text-to-image attentions of the LLM layers are biased, thus bringing inaccuracy, and proposes to utilize the visual saliency of visual tokens as a metric to prune the non-salient tokens. To enhance the pruning effectiveness, some approaches further fine-tune the VLMs. For example, VisionZip(Yang et al., 2024) fine-tunes the MLP projector to improve the alignment for text-to-image attention.

3 Analysis of text-to-image alignment

3.1 Text-to-image similarity distribution in the Pre-LLM layers

FasterVLM comprehensively evaluated the text-to-image attention of the VLMs and revealed the fact that the LLM layers of the VLMs suffer from attention shifts that the subsequent visual tokens attend more attention, compared to the former ones. This nature results in the ineffectiveness of token selection based on text-to-image attention. However, the attention shift is not the case in CLIP (Radford et al., 2021) and the open-vocabulary detection/segmentation tasks (Zheng and Liu, 2024; Bai et al., 2024), we thus assume that the attention layers in the LLM cause this shift, and the original input embeddings including system embeddings, visual embeddings, and the text embeddings do not contain such shift. To validate this, we conduct an experiment on a subset of the llava dataset (Liu et al., 2023) and measure the distribution of the text-to-image similarity of the embedded text tokens and the visual embeddings. We utilize two metrics to measure the alignment: the normalized cosine similarity and the normalized inner product. We visualize the results in Fig. 2, demonstrating no attention shift in the pre-LLM layers. However, the normalized inner product results in significant outliers, which might degrade the model performance. On the contrary, the normalized cosine similarity is more uniform, effectively alleviating the outliers, and therefore more reliable.

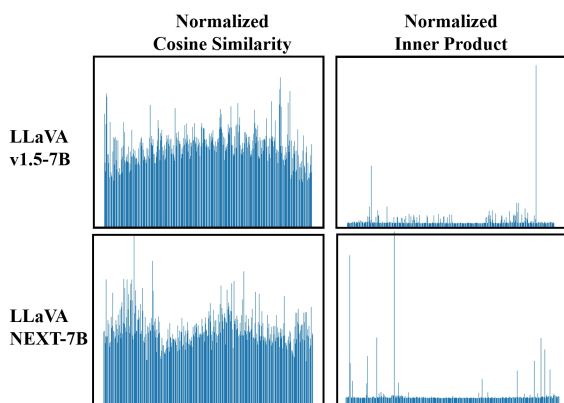


Figure 2: Text-to-image similarity distribution of LLaVA-v1.5-7B and LLaVA-NEXT-vicuna-7B. Compared to the text-to-image attention in the LLM layers, which suffers from attention shift as reported in FasterVLM (Zhang et al., 2024a), the shift does not occur in the pre-LLM layers. We also observe that the cosine similarity could eliminate the outliers.

3.2 Are text embeddings sufficiently aligned with visual embeddings?

After revealing that the text-to-image similarity in the pre-LLM layer does not contain attention shift, we want to know whether the text embeddings are sufficiently aligned with the visual embeddings so that they could be leveraged for informative visual token selection. Since we need to remove the redundant visual tokens, the minimum number of visual tokens to take is utilized as the metric for this validation. Therefore, if at least one image token relative to the prompt is selected, we call it a succeeded selection, and the smallest number of visual tokens to be reserved is utilized to validate the alignment of text embeddings and the visual embeddings. Following FasterVLM, we validate the subset of the llava dataset. We first utilize the state-of-the-art segment-anything-model-2 (Ravi et al., 2024) to segment the objects grounding on the text prompts to generate reliable ground truth prompt-related visual tokens. Then we split the image into 14×14 windows, and calculate the overlapping area of each window to the segmentation mask. We utilize multiple thresholds to determine if an image patch is relative to the text prompt. If the area of overlapping is larger than the threshold, we assume that the patch is relative to the prompt. Then we sort the visual tokens according to the significance measurements (e.g., visual saliency and text-to-image similarity), preserving the top-ranked tokens, until one prompt-related token is included. We visualize the least preserved token number in Fig. 3. Generally, text-to-image similarity takes a smaller number of reserved visual tokens to cover at least one relative visual token, compared with visual saliency, which demonstrates that text-to-image similarity is an effective metric for visual token preservation.

4 Method

4.1 Fixed cross-modality attention mixture

As indicated in the experiments above, solely engaging the visual saliency is insufficient to cover the necessary information for the questions. This suggests that text-image attention is important for information retaining. To address this, we leverage the capacity of both visual saliency and text-image attention for token pruning. A direct solution is to select the top- K tokens according to both visual saliency and text-image similarity. Formally, denote the input text embeddings as $T_E \in$

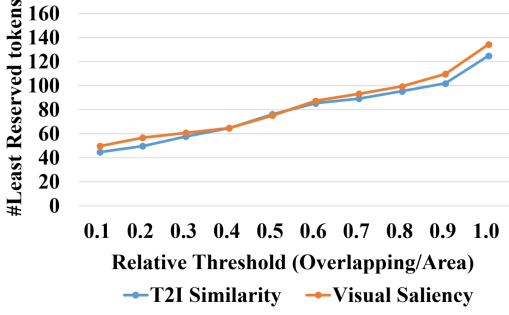


Figure 3: Minimum number of visual tokens to be preserved to select at least one prompt-related visual token, validated on LLaVA-v1.5-7B. Generally, text-to-image similarity takes fewer visual tokens for prompt-related visual token preservation.

$\mathbb{R}^{N_T, D}$, visual embeddings as $T_V \in \mathbb{R}^{N_{img}, N_I, D}$, and the [CLS] token as $C \in \mathbb{R}^{N_{img}, D}$, in which N_T, N_{img}, N_I represent the number of text tokens, images and visual tokens per image. As noted in ViT(), the [CLS] token is utilized for image classification and therefore covers the global information. Therefore, we utilize the attention between the [CLS] token and the visual embeddings to form the visual saliency, since the attention scale indicates the contribution of each visual embedding to the global information. Therefore, the visual saliency could be calculated as follows:

$$S_i^C = \text{Softmax}\left(\frac{C_i W_Q (T_V)_i W_K^T}{\lambda}\right) \quad (1)$$

The similarity between the texts and images could be calculated as follows:

$$S_{i,j}^{T2I} = \max_k \left(\frac{(T_E)_k (T_V)_{i,j}^T}{|(T_E)_k| |(T_V)_{i,j}|} \right), \quad (2)$$

Then we sample the visual tokens as follows:

$$\begin{cases} I_i = \left[\text{argtop-K}(S_{i,:}^C); \text{argtop-K}(S_{i,:}^{T2I}) \right], \\ (\hat{T}_V)_i = (T_V)_{I_i}. \end{cases} \quad (3)$$

4.2 Self-adaptive cross-modality attention mixture (SACMAM)

Although the fixed approach could leverage both global and text-related information, simply mixing them is sub-optimal. To allow the model to determine the preservation of tokens according to the distribution of the visual saliency which highlights the salient image tokens and the text-image similarity which queries the image tokens potentially relative to the question, we propose to allocate the

token budget adaptively, according to the visual saliency and the text-image similarity. As aforementioned, we adopt cosine similarity to select the visual tokens that are aligned with the text. However, the distribution of cosine similarity is not comparable to the visual saliency, which constrains the mixed selection of tokens. To deal with this, we utilize a temperature τ to re-weight the similarity, which could be formally formulated as follows:

$$\tilde{S}_{i,j}^{T2I} = \max_k \left(\text{Softmax}\left(\frac{(T_E)_k (T_V)_{i,j}^T}{|(T_E)_k| |(T_V)_{i,j}| \tau}\right) \right), \quad (4)$$

in which τ is a hyper-parameter. After the re-weight, the text-image similarity becomes comparable to the visual saliency. In the following sections, we suppose the dimensionality of images and tokens per image are merged together for simplicity. In this case, both S^C and \tilde{S}^{T2I} are in the shape of $(N_{img} \times N_I, 1)$. To select the most informative visual tokens within a certain budget with K tokens, a simple solution is to select the top- K tokens as follows:

$$\begin{cases} \hat{I} = \text{top-K}([S^C, \tilde{S}^{T2I}]) \\ \hat{T}_V = (T_V)_{\hat{I}} \end{cases}, \quad (5)$$

which is equivalent to optimizing the following objective:

$$\sum_{i \in \mathcal{I}} \tilde{S}_i^{T2I} + \sum_{j \in \mathcal{J}} S_j^C, \quad \text{s.t.} \quad |\mathcal{I}| + |\mathcal{J}| = K. \quad (6)$$

However, since the distributions of text-image similarity and the visual saliency are different, and only a small group of tokens are selected, it is possible that the model select tokens depends solely on an individual attention score, which is not expected. To deal with this, we utilize the geometric mean of the selected text-to-image similarities and visual saliency to measure the average importance of the selected tokens as follows:

$$\sqrt{\sum_{i \in \mathcal{I}} \tilde{S}_i^{T2I} \sum_{j \in \mathcal{J}} S_j^C}, \quad \text{s.t.} \quad |\mathcal{I}| + |\mathcal{J}| = K, \quad (7)$$

in which \mathcal{I} and \mathcal{J} represent the set of selected visual token indices according to the text-image similarity and visual saliency, respectively. To achieve this, we first sort \tilde{S}^{T2I} and S^C , denote the sorted score as \hat{S}^{T2I} and \hat{S}^C . Then we calculate the cumulative summation of \hat{S}^{T2I} and \hat{S}^C to \mathbf{a} and \mathbf{b} , which could be calculated as follows:

$$\begin{aligned} \mathbf{a}_0 &= 0, \mathbf{b}_0 = 0, \\ \mathbf{a}_i &= \sum_{j=0}^{i-1} \hat{S}_j^{T2I}, \mathbf{b}_i = \sum_{j=0}^{i-1} \hat{S}_j^C, \end{aligned} \quad (8)$$

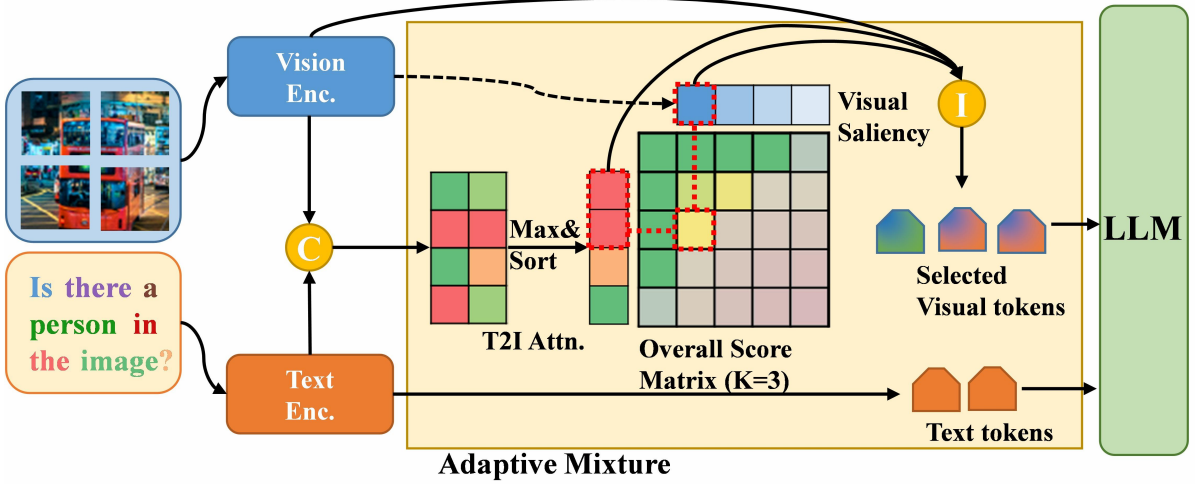


Figure 4: The overall pipeline of the proposed approach. We follow standard VLMs to encode the input image and text. We utilize text-to-image similarity to formulate T2I attention and integrate the attention weights of image tokens by calculating the maximum value. We obtain the overall significance by mixing the T2I attention and visual saliency extracted from the vision encoder and selecting the most informative visual tokens accordingly.

Then we calculate the overall metrics as follows:

$$O = \mathbf{a}\mathbf{b}^T. \quad (9)$$

In order that the invalid indices will not be chosen, we utilize a mask M to set the elements of O corresponding to such indices to zero. Specifically, the mask M could be calculated as follows:

$$M_{i,j} = \begin{cases} 1, & i + j \leq K \\ 0, & \text{otherwise} \end{cases}. \quad (10)$$

Then the number of tokens selected by text-to-image similarity and visual saliency could be determined as follows:

$$U, V = \underset{i,j}{\operatorname{argmax}} \{(O \otimes M)_{i,j}\}. \quad (11)$$

After determining the number of tokens selected depending on each significance measurement, we choose the top-valued indices for visual token indexing as follows:

$$\begin{cases} \mathcal{I} = \{i | \operatorname{rank}(S_i^{T2I}) \leq U\} \\ \mathcal{J} = \{j | \operatorname{rank}(S_j^C) \leq V\} \end{cases}. \quad (12)$$

The selected visual tokens could finally be formulated as $\{(T_V)_k\}_{k \in \mathcal{I} \cup \mathcal{J}}$. Note that the selected tokens are sorted according to their original position on the image to maintain the correct spatial relationship. We allow replicated visual tokens for simplicity.

5 Experiments

5.1 Implementation details

We validate the proposed approach on the LLaVA-v1.5 and LLaVA-NEXT models. We include widely utilized VLM benchmarks to evaluate our method, including GQA (Hudson and Manning, 2019), SQA (Lu et al., 2022), MME (Fu et al., 2024a), MMBench (Liu et al., 2025), MMVet (Yu et al., 2023), TextVQA (Singh et al., 2019) and Pope (Yifan et al., 2023). All experiments are conducted on the NVIDIA A100-80G GPU.

5.2 Comparison with SOTA approaches

We first compare the proposed approach with other state-of-the-art training-free token pruning methods. Since different research works may include different benchmark datasets, and utilize different reduction rates and metrics (for example, VisionZip utilizes the summation of perception and cognition score, while the FasterVLM only includes the perception score), we separate the comparisons accordingly in Tab. 1 for clear comparison on LLaVA-NEXT-vicuna-7B model. We also show the effectiveness of other VLMs briefly in Tab. 2, and the detailed comparison is demonstrated in the Appendix. Compared with the other methods, the proposed approach achieves SOTA performance compared with the training-free approaches and even exceeds the fine-tuned methods. Compared with the other token-pruning methods, our method shows stronger robustness in scenarios where less than 10% visual

Table 1: Comparison with SOTA approaches on LLaVA-NEXT-7B. † means that we report both the perception-only score and the summation of the perception score and the cognition score in parenthesis. ‡ represents the model is fine-tuned.

Method	GQA	SQA-IMG	TextVQA	POPE	MME†	MMB	MM-Vet	Average
LLaVA-NEXT-7B	62.93	69.66	59.59	86.32	1513.78 (1842.00)	67.70	42.60	100.00%
Reduction Rate \approx 75%								
FastV	60.38	69.81	58.39	83.09	1477.31	65.64	41.10	97.35%
SparseVLM	60.88	67.48	58.08	70.99	1446.10	63.83	38.00	93.19%
FaseterVLM	61.31	68.82	59.33	85.50	1480.68	67.35	40.40	98.14%
Ours	62.04	69.31	58.37	87.20	1509.36	67.35	39.70	98.49%
VisionZip	61.30	68.10	60.20	86.30	1702.00	66.30		97.75%
Ours	62.04	69.31	58.37	87.20	1810.07	67.35		99.13%
VisionZip+FT‡	62.40	67.90	60.80	87.60	1778.00	65.90		99.00%
Reduction Rate \approx 90%								
FastV	55.86	69.26	55.69	71.66	1282.86	61.60	22.70	84.81%
SparseVLM	56.12	68.62	51.97	63.23	1332.22	54.47	24.70	82.08%
FaseterVLM	58.12	68.12	57.57	80.00	1370.11	63.32	35.70	92.47%
Ours	60.65	68.57	57.09	85.98	1503.25	66.32	36.00	96.00%
VisionZip	59.30	67.30	58.90	82.10	1702.00	63.10		95.07%
Ours	60.65	68.57	57.09	85.98	1812.89	66.32		97.77%
VisionZip+FT‡	61.00	67.50	59.30	86.20	1770.00	64.40		97.40%
Reduction Rate \approx 95%								
FastV	49.83	68.52	51.85	51.66	1079.46	54.90	21.90	75.46%
FaseterVLM	54.73	68.86	55.97	72.89	1225.96	60.48	31.90	87.06%
Ours	58.53	68.91	55.11	85.25	1452.91	65.20	36.20	94.35%
VisionZip	55.50	68.30	56.20	74.80	1630.00	60.10		90.75%
Ours	58.53	68.91	55.11	85.25	1736.12	65.20		95.62%
VisionZip+FT‡	58.20	67.50	57.30	83.40	1699.00	63.90		94.80%

tokens are preserved. Specifically, for the LLaVA-NEXT-vicuna-7B model, with the 95% reduction rate, the proposed approach exceeds the training-free methods by 5.0%, and the fine-tuned VisionZip by 0.8%. For the LLaVA-NEXT-13B model, the proposed approach also exceeds the fine-tuned VisionZip by 1.9% (Appendix). These results demonstrate the effectiveness of the proposed approach.

5.3 Ablation study

Overall ablation We conduct an overall ablation study of the proposed approach. As demonstrated in Tab. 3, the T2I attention significantly boosts the model performance, especially when the number of retained tokens is small. The proposed adaptive mixture could further boost the model by 1.0% for a larger than 90% reduction rate.

Table 2: Comparison with SOTA approaches on VLM benchmarks. The proposed method achieves state-of-the-art performance, especially for a large reduction rate.

Method	Reduction Rate		
	75%	90%	95%
LLaVA-1.5-7B			
FastV	94.67%	86.26%	72.48%
FitPrune	96.22%	81.62%	/
SparseVLM	93.22%	78.87%	65.85%
FaseterVLM	98.32%	92.91%	87.76%
Ours	97.83%	93.59%	88.32%
LLaVA-NEXT-13B			
FaseterVLM	97.57%	92.79%	86.52%
Ours	97.75%	95.40%	93.14%

Table 3: Ablation study of main modules on LLaVA-NEXT-vicuna-7B

Model	#Tokens		
	720	288	144
Ours	98.49%	96.00%	94.35%
-Adaptive Mixture	98.40%	94.89%	92.62%
-T2I Attention	98.18%	92.47%	87.06%

Detailed ablation results on specific dataset To further understand the influence of the proposed mechanisms, we validate the model on two datasets: Pope and TextVQA. We validate the method on these datasets because we empirically find that the proposed approach achieves superior performance on the Pope dataset, but is less effective on the TextVQA. The results are demonstrated in Tab. 4, 5. Solely leverages visual saliency on the Pope dataset resulting in a significant degradation of performance, while the T2I similarity is much more effective in comparison. The simple mixture approach exceeds the visual saliency-only method, while slightly beneath the T2I-only. On the contrary, for the TextVQA dataset, the T2I-only method resulted in obvious performance degradation, and the simple mixture approach also resulted in a performance drop. Compared with the simple mixture, the proposed adaptive mixture significantly reduces the performance degradation on both datasets, demonstrating its robustness across different tasks.

Table 4: Ablation study on the Pope dataset. ‘‘SAC-MAM’’, ‘‘T2I’’ and ‘‘VS’’ demonstrate self-adaptive cross-modality attention mixture, text-to-image similarity and visual saliency, respectively.

SACMAM	T2I	VS	#Tokens		
			720	288	144
×	×	✓	85.50	80.00	72.89
×	✓	×	87.11	86.21	85.12
×	✓	✓	87.07	85.52	84.04
✓	✓	✓	87.20	85.98	85.25

Attention dependency analysis We further analyze the attention dependency of different datasets and demonstrate the results in Fig. 5. If the curve is of \mathcal{I}/K left-oriented on the figure, the model is less dependent on the text-to-image similarity. On the contrary, the model is less dependent on visual saliency, if the model relies more on it. We

Table 5: Ablation study on the TextVQA dataset. ‘‘SAC-MAM’’, ‘‘T2I’’ and ‘‘VS’’ demonstrate self-adaptive cross-modality attention mixture, text-to-image similarity and visual saliency, respectively.

SACMAM	T2I	VS	#Tokens		
			720	288	144
×	×	✓	59.33	57.57	55.97
×	✓	×	57.47	54.43	51.57
×	✓	✓	57.27	55.76	53.36
✓	✓	✓	58.37	57.09	55.11

found that the model tends to rely more on visual saliency for tasks that are not related to natural images (TextVQA). This might be because the visual embeddings of the text layouts are not sufficiently aligned with text embeddings, which results in the ineffectiveness of text-to-image similarity in such scenarios. On the contrary, the proposed approach solves the tasks in the POPE dataset, which could be sufficiently solved by text-to-image similarity, depending more on it. This result demonstrates that the proposed self-adaptive cross-modality attention mixture could effectively determine the reliance on visual saliency and text-to-image similarity, boosting the performance of the VLMs.

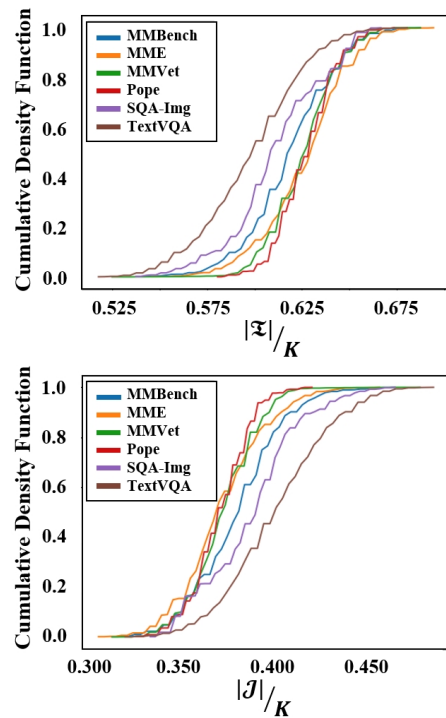


Figure 5: The cumulative density function (CDF) of the partition of T2I-oriented tokens (\mathcal{I}) and visual saliency-oriented tokens (\mathcal{J}) on benchmark datasets.

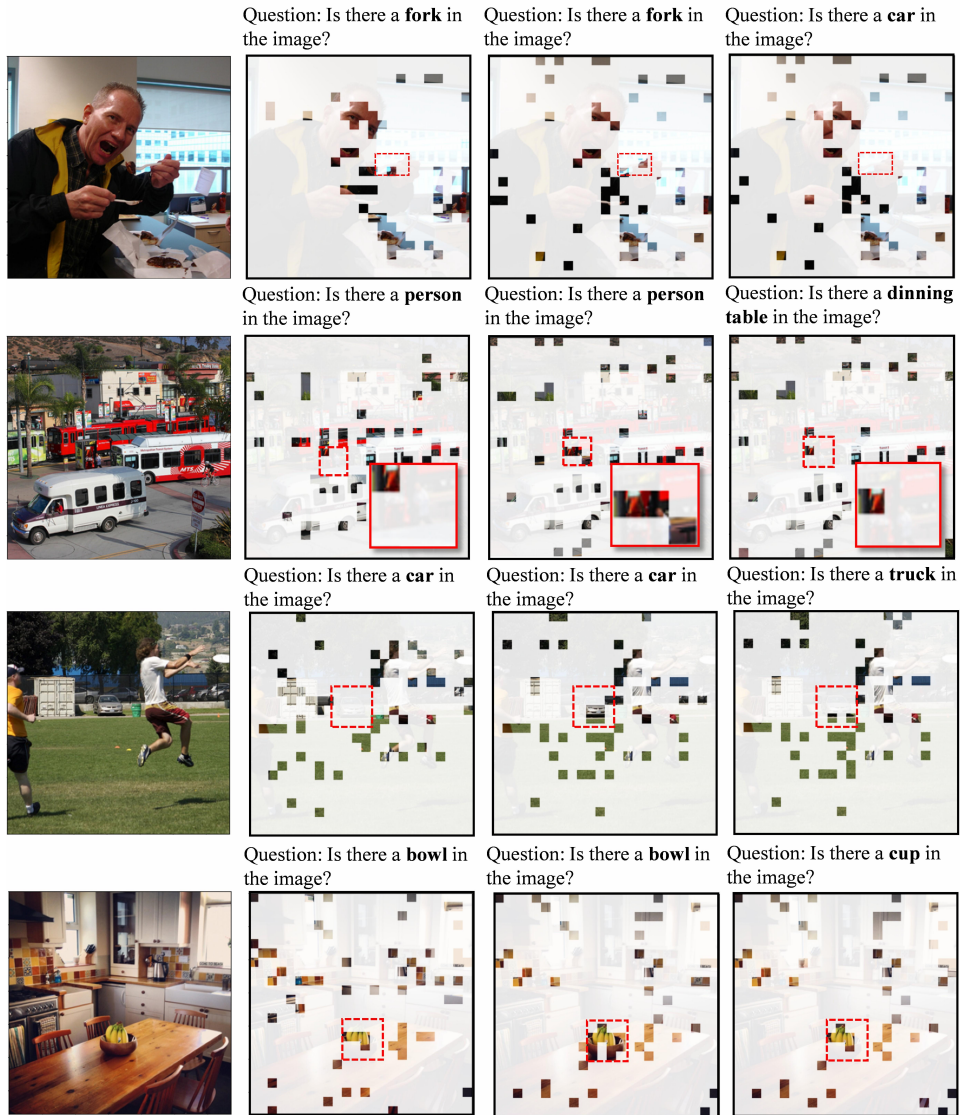


Figure 6: The visualization of selected tokens of FasterVLM (column 2) and the proposed approach (columns 3 and 4). The transparent patches are not selected. Compared with the FasterVLM, the proposed approach managed to focus on question-related tokens. Better zoom in for visualization.

5.4 Visualization of selected tokens

We further visualize the selected tokens of the FasterVLM and the proposed approach in Fig. 6. Since the FasterVLM approach is text-agnostic, the selected visual tokens are consistent with a certain input image, which results in the VLM only accessing the salient objects, and failing to allocate the cases in which the user prompts are about non-salient objects in the image. On the contrary, the proposed approach effectively leverages the strength of both visual saliency and text-to-image similarity. As depicted in the figure, the proposed approach could draw attention to the detailed information according to the text prompts, and remove it when not relative.

6 Conclusion

In this work, we first analyze the text-to-image similarity in the pre-LLM layers and reveal that the original text embeddings are sufficiently aligned with the visual embeddings for natural image VQA, which suggests that the token pruning before the LLM self-attention is potentially effective. Then we propose an adaptive mixture of visual saliency and text-to-image similarity to select informative visual tokens without introducing additional computational cost. Extensive experiments demonstrate that the proposed approach significantly strengthens the robustness of VLMs for acceleration, and achieves state-of-the-art performance compared with the other approaches.

7 Limitations

In this section, we discuss the limitations of the proposed approach. Firstly, although the proposed approach demonstrates the effectiveness of visual token pruning, it relies on sufficient alignment of the text embeddings and visual information, which needs further validation for the native VLMs that utilize VQ-VAE models to generate discrete visual tokens. Second, from visualization, we could still find that there are plenty of redundant visual tokens that are irrelevant to the input prompt. Further exploration of visual information smoothing and filtering is needed to enhance the VLMs' efficiency.

References

- Jinze Bai, Shuai Bai, Shusheng Yang, Shijie Wang, Sinan Tan, Peng Wang, Junyang Lin, Chang Zhou, and Jingren Zhou. 2023. Qwen-vl: A versatile vision-language model for understanding, localization, text reading, and beyond. *arXiv preprint arXiv:2308.12966*.
- Sule Bai, Yong Liu, Yifei Han, Haoji Zhang, and Yansong Tang. 2024. Self-calibrated clip for training-free open-vocabulary segmentation. *arXiv preprint arXiv:2411.15869*.
- Liang Chen, Haozhe Zhao, Tianyu Liu, Shuai Bai, Junyang Lin, Chang Zhou, and Baobao Chang. 2024a. An image is worth 1/2 tokens after layer 2: Plug-and-play inference acceleration for large vision-language models. *Preprint*, arXiv:2403.06764.
- Zhe Chen, Weiyun Wang, Yue Cao, Yangzhou Liu, Zhangwei Gao, Erfei Cui, Jinguo Zhu, Shenglong Ye, Hao Tian, Zhaoyang Liu, et al. 2024b. Expanding performance boundaries of open-source multimodal models with model, data, and test-time scaling. *arXiv preprint arXiv:2412.05271*.
- Zhe Chen, Jiannan Wu, Wenhai Wang, Weijie Su, Guo Chen, Sen Xing, Muyan Zhong, Qinglong Zhang, Xizhou Zhu, Lewei Lu, et al. 2024c. Internvl: Scaling up vision foundation models and aligning for generic visual-linguistic tasks. In *Proceedings of the IEEE/CVF Conference on Computer Vision and Pattern Recognition*, pages 24185–24198.
- Chaoyou Fu, Peixian Chen, Yunhang Shen, Yulei Qin, Mengdan Zhang, Xu Lin, Jinrui Yang, Xiawu Zheng, Ke Li, Xing Sun, Yunsheng Wu, and Rongrong Ji. 2024a. Mme: A comprehensive evaluation benchmark for multimodal large language models. *Preprint*, arXiv:2306.13394.
- Qichen Fu, Minsik Cho, Thomas Merth, Sachin Mehta, Mohammad Rastegari, and Mahyar Najibi. 2024b. Lazyllm: Dynamic token pruning for efficient long context llm inference. *arXiv preprint arXiv:2407.14057*.
- Drew A Hudson and Christopher D Manning. 2019. Gqa: A new dataset for real-world visual reasoning and compositional question answering. In *Proceedings of the IEEE/CVF conference on computer vision and pattern recognition*, pages 6700–6709.
- Sehoon Kim, Sheng Shen, David Thorsley, Amir Ghohami, Woosuk Kwon, Joseph Hassoun, and Kurt Keutzer. 2022. Learned token pruning for transformers. In *Proceedings of the 28th ACM SIGKDD Conference on Knowledge Discovery and Data Mining*, pages 784–794.
- Ji Lin, Hongxu Yin, Wei Ping, Yao Lu, Pavlo Molchanov, Andrew Tao, Huihui Mao, Jan Kautz, Mohammad Shoeybi, and Song Han. 2023. Vila: On pre-training for visual language models. *Preprint*, arXiv:2312.07533.
- Haotian Liu, Chunyuan Li, Yuheng Li, Bo Li, Yuanhan Zhang, Sheng Shen, and Yong Jae Lee. 2024. Llava-next: Improved reasoning, ocr, and world knowledge.
- Haotian Liu, Chunyuan Li, Qingyang Wu, and Yong Jae Lee. 2023. Visual instruction tuning.
- Yuan Liu, Haodong Duan, Yuanhan Zhang, Bo Li, Songyang Zhang, Wangbo Zhao, Yike Yuan, Jiaqi Wang, Conghui He, Ziwei Liu, et al. 2025. Mmbench: Is your multi-modal model an all-around player? In *European conference on computer vision*, pages 216–233. Springer.
- Pan Lu, Swaroop Mishra, Tanglin Xia, Liang Qiu, Kai-Wei Chang, Song-Chun Zhu, Oyvind Tafjord, Peter Clark, and Ashwin Kalyan. 2022. Learn to explain: Multimodal reasoning via thought chains for science question answering. *Advances in Neural Information Processing Systems*, 35:2507–2521.
- Alec Radford, Jong Wook Kim, Chris Hallacy, Aditya Ramesh, Gabriel Goh, Sandhini Agarwal, Girish Sastry, Amanda Askell, Pamela Mishkin, Jack Clark, et al. 2021. Learning transferable visual models from natural language supervision. In *International conference on machine learning*, pages 8748–8763. PMLR.
- Nikhila Ravi, Valentin Gabeur, Yuan-Ting Hu, Ronghang Hu, Chaitanya Ryali, Tengyu Ma, Haitham Khedr, Roman Rädle, Chloe Rolland, Laura Gustafson, Eric Mintun, Junting Pan, Kalyan Vasudev Alwala, Nicolas Carion, Chao-Yuan Wu, Ross Girshick, Piotr Dollár, and Christoph Feichtenhofer. 2024. Sam 2: Segment anything in images and videos. *arXiv preprint arXiv:2408.00714*.
- Amanpreet Singh, Vivek Natarajan, Meet Shah, Yu Jiang, Xinlei Chen, Dhruv Batra, Devi Parikh, and Marcus Rohrbach. 2019. Towards vqa models that can read. In *Proceedings of the IEEE/CVF conference on computer vision and pattern recognition*, pages 8317–8326.
- Hongjie Wang, Bhishma Dedhia, and Niraj K Jha. 2024. Zero-tprune: Zero-shot token pruning through leveraging of the attention graph in pre-trained transformers. In *Proceedings of the IEEE/CVF Conference*

on *Computer Vision and Pattern Recognition*, pages 16070–16079.

Senqiao Yang, Yukang Chen, Zhuotao Tian, Chengyao Wang, Jingyao Li, Bei Yu, and Jiaya Jia. 2024. Visionzip: Longer is better but not necessary in vision language models. *arXiv preprint arXiv:2412.04467*.

Weihao Ye, Qiong Wu, Wenhao Lin, and Yiyi Zhou. 2024. Fit and prune: Fast and training-free visual token pruning for multi-modal large language models. *arXiv preprint arXiv:2409.10197*.

Li Yifan, Du Yifan, Zhou Kun, Wang Jinpeng, Xin Zhao Wayne, and Ji-Rong Wen. 2023. [Evaluating object hallucination in large vision-language models](#). In *The 2023 Conference on Empirical Methods in Natural Language Processing*.

Weihao Yu, Zhengyuan Yang, Linjie Li, Jianfeng Wang, Kevin Lin, Zicheng Liu, Xinchao Wang, and Lijuan Wang. 2023. Mm-vet: Evaluating large multimodal models for integrated capabilities. *arXiv preprint arXiv:2308.02490*.

Qizhe Zhang, Aosong Cheng, Ming Lu, Zhiyong Zhuo, MinQi Wang, Jiajun Cao, Shaobo Guo, Qi She, and Shanghang Zhang. 2024a. [cls] attention is all you need for training-free visual token pruning: Make vlm inference faster. *arXiv preprint arXiv:2412.01818*.

Yuan Zhang, Chun-Kai Fan, Junpeng Ma, Wenzhao Zheng, Tao Huang, Kuan Cheng, Denis Gudovskiy, Tomoyuki Okuno, Yohei Nakata, Kurt Keutzer, et al. 2024b. Sparsevlm: Visual token sparsification for efficient vision-language model inference. *arXiv preprint arXiv:2410.04417*.

Yanhao Zheng and Kai Liu. 2024. Training-free boost for open-vocabulary object detection with confidence aggregation. *arXiv preprint arXiv:2404.08603*.

A Detailed comparison on LLaVA-v1.5 7B and LLaVA-NEXT 13B

We show a detailed comparison of the token pruning methods on LLaVA-v1.5-7B and LLaVA-NEXT-13B in Tab. 6 and 7. For LLaVA-NEXT-13B, the proposed AdaFV achieves state-of-the-art performance across all the involved reduction rates and achieves even stronger performance than the fine-tuned VisionZip. AdaFV also achieves comparable performance to other state-of-the-art methods.

Table 6: Comparison with SOTA approaches on LLaVA-NEXT-13B. † means that we report both the perception-only score and the summation of the perception score and the cognition score in parenthesis. ‡ represents the model is fine-tuned.

Method	GQA	SQA-IMG	TextVQA	POPE	MME	MMB	MM-Vet	Average
LLaVA-NEXT-13B	65.40	73.60	67.10	86.20	1575.00 (1901.00)	70.00	48.40	100.00%
Reduction Rate \approx 75%								
FaseterVLM	63.05	72.88	61.67	85.27	1548.06	69.50	48.00	97.57%
Ours	64.26	73.33	61.93	86.70	1599.80	70.10	44.40	97.75%
VisionZip	63.00	71.20	62.20	85.70	1871.00	68.60		96.93%
Ours	64.26	73.33	61.93	86.70	1938.72	70.10		98.82%
VisionZip+FT [‡]	63.70	73.20	64.40	86.30	1829.00	66.60		97.38%
Reduction Rate \approx 90%								
FaseterVLM	59.68	71.24	60.14	80.39	1470.98	67.61	42.90	92.79%
Ours	62.78	73.53	59.76	85.79	1603.05	69.67	39.70	95.40%
VisionZip	60.70	70.30	60.90	82.00	1805.00	67.20		94.19%
Ours	62.78	73.53	59.76	85.79	1912.69	69.67		97.44%
VisionZip+FT [‡]	62.50	72.70	63.20	85.70	1861.00	66.90		96.90%
Reduction Rate \approx 95%								
FaseterVLM	56.14	70.40	58.43	73.81	1388.44	64.69	34.30	86.52%
Ours	60.97	72.68	58.05	84.76	1557.43	68.56	37.90	93.14%
VisionZip	57.80	69.30	58.40	76.60	1739.00	64.90		90.44%
Ours	60.97	72.68	58.05	84.76	1867.07	68.56		95.50%
VisionZip+FT [‡]	59.70	72.00	60.80	84.00	1766.00	65.30		93.89%

Table 7: Comparison with SOTA approaches on LLaVA-v1.5-7B. [†] means that we report both the perception-only score and the summation of the perception score and the cognition score in parenthesis. [‡] represents the model is fine-tuned.

Method	GQA	SQA-IMG	TextVQA	POPE	MME	MMB	MM-Vet	Average
LLaVA-1.5-7B	61.94	69.51	58.21	85.88	1506.47 (1862.00)	64.69	31.30	100.00%
Reduction Rate \approx 75%								
FastV	56.58	69.11	57.38	73.74	1463.39	64.00	28.60	94.67%
FitPrune	59.38	69.01	56.49	80.75	1472.86	63.92	28.40	96.22%
SparseVLM	55.11	69.36	55.99	77.57	1351.65	59.54	29.90	93.22%
FaseterVLM	58.34	67.92	57.07	83.46	1433.76	62.54	34.20	98.32%
Ours	58.38	69.31	56.66	84.72	1432.68	62.28	32.40	97.83%
VisionZip	57.60	68.90	56.80	83.20	1761.70	62.00	30.00	96.12%
Ours	58.38	69.31	56.66	84.72	1762.32	62.28	32.40	97.77%
VisionZip+FT	58.90	68.30	57.00	83.70	1823.00	62.60	32.90	98.36%
Reduction Rate \approx 90%								
FastV	51.20	69.81	54.75	57.30	1210.36	59.97	27.20	86.26%
FitPrune	49.96	68.22	56.49	53.81	1147.46	56.27	21.80	81.62%
SparseVLM	48.86	67.23	55.99	65.82	1030.61	49.05	18.60	78.87%
FaseterVLM	54.91	68.91	55.28	75.85	1348.63	60.57	30.10	92.91%
Ours	55.30	68.82	54.53	82.33	1368.28	60.30	29.20	93.59%
VisionZip	55.10	69.00	55.50	77.00	1690.00	60.10	31.70	94.02%
Ours	55.30	68.82	54.53	82.33	1695.42	60.30	29.20	93.63%
VisionZip+FT	58.90	68.80	56.00	80.90	1756.00	61.50	30.20	95.76%
Reduction Rate \approx 95%								
FastV	46.03	70.00	51.56	35.47	971.56	50.17	18.90	72.48%
FitPrune	43.60	68.32	46.75	31.17	855.21	39.69	18.00	65.85%
FaseterVLM	51.51	69.56	53.09	67.24	1254.80	58.51	27.50	87.76%
Ours	52.96	68.42	51.89	78.04	1313.36	58.51	24.00	88.32%